

## Thermodynamic analysis of interactions between Ti–Al alloys and oxide ceramics

CUI Ren-jie, TANG Xiao-xia, GAO Ming, ZHANG Hu, GONG Sheng-kai

Key Laboratory of Aerospace Materials and Performance (Ministry of Education),  
School of Materials Science and Engineering, Beihang University, Beijing 100191, China

Received 18 May 2011; accepted 10 October 2011

**Abstract:** The thermodynamics of interactions between various oxides (CaO, MgO, Al<sub>2</sub>O<sub>3</sub> and Y<sub>2</sub>O<sub>3</sub>) and molten Ti and Ti alloys was investigated. The dissolution mechanism of oxides in molten Ti alloys was provided and the stability of oxides in molten Ti alloys was investigated and predicted by thermodynamic analysis. Interactions between oxides and Ti–Al melts were studied by oxide crucible melting experiments. By quantitative analysis, it is indicated that impurity contents in alloys are proportionally decreased with increasing the Al content in alloys and decreasing the melt temperature, which is in agreement with the results of the predicting thermodynamic stability.

**Key words:** Ti alloys; thermodynamics; oxide ceramics; interaction

### 1 Introduction

Ti alloy is an important structural material, due to its high specific strength, good biocompatibility, high corrosion resistance and many other advantages. At the present stage, Ti alloy is a promising metallic material and its production is widely used in emerging markets, such as aerospace, military, petroleumical industry, textile, biomedical devices, automotive industry, and sports [1,2]. TiAl alloys have attracted attention as potential candidates for high-temperature structural applications in the aerospace and military [3]. However, the main factors to limit the manufacture of mass market Ti alloy components are the high reactivity of Ti alloys with crucible/mould refractory materials at high temperatures. When the interactions between the alloys and crucible/mould materials occur, the microstructure and properties of the castings will be affected. Therefore, it is necessary to investigate the interactions between refractory materials and Ti alloy melts and select suitable refractory materials as crucibles or moulds for melting or casting the alloy.

At present, many researchers have investigated interactions between Ti alloy melts and refractory

materials, including borides, carbides, sulfide, nitride and oxide [4,5]. The results show that the oxide family of materials receives the most attention, due to its low cost, high melting point and high refractoriness. Moreover, the Gibbs free energy diagram of oxides can also be useful for comparison of the relative stability of oxides. However, SAHA et al [2] experimentally found that the stability of various oxides against Ti melts is not consistent with the free energy of formation of these oxides, indicating that the standard free energy diagram does not provide a correct picture of the reactivity of oxides with liquid metal. Researches so far indicate that the solution effects of oxides in liquid metal need to be taken into consideration to obtain a more realistic picture. Many researchers [6–10] have studied the thermodynamic stability of oxides against Ti alloy melts, but mainly focus on experimental aspects, whose cost is high while accuracy is low. Therefore, it is instructive to theoretically predict the thermodynamic stability of oxides and investigate interactions between Ti alloy melts and oxides.

In this study, the dissolution mechanism of oxides in molten Ti alloys was provided and the stability of various oxides were investigated and predicted by thermodynamic analysis. Moreover, melting experiments

of Ti–xAl ( $x=0$ , 25%, 43%, 47%, mole fraction) alloys were performed to study the oxide–melt interaction. The melting effect was quantitatively analyzed and compared with the oxide stability.

## 2 Experimental

### 2.1 Model

In TiAl melts, the chemical reactivity of the melts depends on the chemical activities of Ti and Al elements in the melts. According to the basic thermodynamics of alloy melts and the previous theoretical and experimental research on TiAl melts [11–13], the activities of Ti and Al in TiAl melts can be quantitatively calculated, which provides the basis for the study of the interaction mechanism between TiAl melts and the oxide materials. In binary  $i-j$  systems, the relationship between the partial molar excess free energy ( $\bar{G}_i^E$ ) and the activity coefficient ( $\gamma_i$ ) of component  $i$  is expressed as follows:

$$\bar{G}_i^E = RT \ln \gamma_i \quad (1)$$

and the molar excess free energy is defined as:

$$\bar{G}_i^E = G_{ij}^E + (1-x_i) \frac{\partial G_{ij}^E}{\partial x_i} \quad (2)$$

where  $x_i$  is the mole fraction of component  $i$ ;  $\bar{G}_i^E$  is the partial molar excess free energy of component  $i$ ;  $G_{ij}^E$  is the excess free energy of binary  $i-j$  system and can be defined as:

$$G_{ij}^E = H_{ij}^E - TS_{ij}^E = \Delta H_{ij} - TS_{ij}^E \quad (3)$$

in which  $\Delta H_{ij}$  is the enthalpy of formation during the alloying process between component  $i$  and  $j$ ;  $S_{ij}^E$  is the excess entropy of components  $i$  and  $j$ . A connection between  $\Delta H_{ij}$  and  $S_{ij}^E$  can be written as [14]:

$$S_{ij}^E \approx \frac{1}{10} \times \Delta H_{ij} \left( \frac{1}{T_{mi}} + \frac{1}{T_{mj}} \right) \quad (4)$$

$$G_{ij}^E = \alpha_{ij} \times \Delta H_{ij} \quad (5)$$

where

$$\alpha_{ij} = 1 - \frac{1}{10} \times T \left( \frac{1}{T_{mi}} + \frac{1}{T_{mj}} \right),$$

$T_{mi}$  and  $T_{mj}$  are melting points of the components  $i$  and  $j$ , respectively. The formation enthalpy  $\Delta H_{ij}$  can be calculated from Miedema model [15]. The Miedema model of formation of binary alloys has been widely applied to forecasting the formation enthalpy of binary metal solutions. Many researchers have studied the chemical activity coefficient of the components in binary systems based on this model, and the calculated results are identical to the experimental data [11,12]. According to the Miedema model, the formation enthalpy of binary  $i-j$  solutions  $\Delta H_{ij}$  can be written as:

$$\begin{aligned} \Delta H_{ij} = & f_{ij} x_i [1 + \mu_i x_j (\phi_i - \phi_j)] x_j [1 + \mu_j x_i (\phi_j - \phi_i)] / \\ & \{x_i V_i^{2/3} [1 + \mu_i x_i (\phi_i - \phi_j)] + \\ & x_j V_j^{2/3} [1 + \mu_j x_i (\phi_j - \phi_i)]\} \end{aligned} \quad (6)$$

where,

$f_{ij} = 2PV_i^{2/3}V_j^{2/3} [q/p(\Delta n_{ws})^2 - (\Delta\phi)^2 - \alpha(r/p)] / \left[ (n_{ws}^{1/3})_i^{-1} + (n_{ws}^{1/3})_j^{-1} \right]$ ,  $x_i$  and  $x_j$  are the mole fraction of  $i$  and  $j$ , respectively;  $V_i$  and  $V_j$  are the mole volumes of  $i$  and  $j$ , respectively;  $(n_{ws})_i$  and  $(n_{ws})_j$  are the electronic density of  $i$  and  $j$ , respectively;  $\phi_i$ ,  $\phi_j$  are electronic charges of  $i$  and  $j$ , respectively;  $p$ ,  $q$ ,  $r$ ,  $\alpha$  are the experimental constants, where  $q/p=9.4$ ,  $\alpha=0.94$ ,  $p=12.3$  for binary TiAl melts [12].

Using Eqs. (1)–(6), the calculation model for chemical activity coefficient ( $\gamma_i$ ) of the component  $i$  in binary  $i-j$  systems is expressed as:

$$\begin{aligned} \ln \gamma_i = & \frac{\alpha_{ij} \cdot \Delta H_{ij}}{RT} \{1 + (1-x_i) \left\{ \frac{1}{x_i} - \frac{1}{1-x_i} - \right. \\ & \left. \frac{\mu_i (\phi_i - \phi_j)}{V_i^{2/3} [1 + \mu_i (1-x_j) (\phi_i - \phi_j)]} + \frac{1 + \mu_j (\phi_j - \phi_i)}{1 + \mu_j x_i (\phi_j - \phi_i)} - \right. \\ & \left. \{V_i^{2/3} [1 + \mu_i (1-2x_j) (\phi_i - \phi_j)] + \right. \\ & \left. V_j^{2/3} [-1 + \mu_j (1-2x_i) (\phi_j - \phi_i)]\} / \right. \\ & \left. \{x_i V_i^{2/3} [1 + \mu_i (1-2x_j) (\phi_i - \phi_j)] + \right. \\ & \left. (1-x_i) V_j^{2/3} [-1 + \mu_j (1-2x_i) (\phi_j - \phi_i)]\} \right\} \} \end{aligned} \quad (7)$$

### 2.2 Melting experiment

In this work, TiAl alloys with nominal compositions of Ti–xAl ( $x=0$ , 25%, 43%, 47%, mole fraction) were produced from pure elements, titanium sponge (mass fraction, 99.76%) and high purity Al ingot (99.99%). Special care was taken to clean the raw materials, using acetone solution in an ultrasonic bath. After cleaning, they were dried at 150 °C for 120 min. The master alloy was prepared as a button of 1000 g by arc melting in a high purity argon atmosphere using a non-consumable tungsten electrode. The button was melted and turned five times to promote homogeneity. In order to prepare samples that would fit into the crucibles, the arc-melted button was cut to give master alloy samples with dimensions of 15 mm (diameter)×20 mm (height) using electrical discharge machining (EDM). Before the melting experiments, these samples were ground, cleaned and dried using the same procedure as described for the raw materials.

Melting was performed using a modified Bridgman furnace equipped with an yttria crucible (20 mm (out diameter)×15 mm (inner diameter)×20 mm (inner height), purity 99.9%), as shown in Fig. 1. Before the heating cycle, the furnace chamber was evacuated down to

$6 \times 10^{-3}$  Pa. After switching on the furnace power and heating up to 400 °C (keep evacuating), the furnace was backfilled with high purity argon ( $\phi(O_2) < 2 \times 10^{-6}$ ,  $\phi(N_2) < 5 \times 10^{-6}$ ,  $\phi(H_2) < 1 \times 10^{-6}$ ,  $\phi(H_2O) < 1 \times 10^{-6}$ ,  $\phi(CH_4) < 1 \times 10^{-6}$ ) up to 0.05 MPa, in order to reduce the oxygen and hydrosphere contents to a minimum level and avoid the evaporation of alloy components. After 40 min since the start of the heating cycle, the temperature reached 1400 °C. Afterwards, the heating rate was increased in order to reach the desired temperature as fast as possible. After reaching the temperature measured and controlled by a thermocouple A (WRe5–WRe26, Fig. 1) combined with an infrared pyrometer, the melt inside the crucible was stabilized at this temperature for 600 s in the furnace and then the furnace power was switched off. Finally, the crucible containing the cast ingot was removed from the furnace at a temperature of about 50 °C.

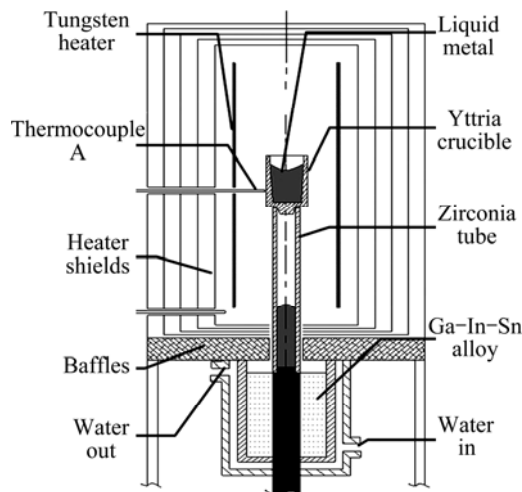


**Fig. 1** Schematic diagram of modified Bridgman furnace equipped with yttria crucible

### 2.3 Characterization

The total oxygen contents of all ingots that were exposed to the yttria crucibles were measured by the inert gas infrared-thermal conductivity technique (IGI, LECO TC-436), with a measuring accuracy of  $\pm 1 \times 10^{-6}$ . For each ingot, two 0.8–1.2 g cylindrical bars parallel to the longitudinal axis of the ingot were taken at a distance of 3 mm from its surface. After being ground to a final mesh size of 120#, cleaned and dried using the same procedure as described for the raw materials, these bars were used for chemical analysis.

## 3 Results and discussion

### 3.1 Chemical activity of components in binary TiAl alloys

In order to study the thermodynamic stability of oxides against TiAl melts, the activity coefficients of the

components Ti and Al as a function of temperature need to be known. The basic properties of some chemical elements and parameters used for calculations are listed in Table 1. By Eq. (7), the activity coefficients of Ti and Al in TiAl melts with different Al contents are calculated in a temperature range of 1800–2300 K, respectively. The activity coefficient — temperature — composition relationship for Ti and Al is shown in Fig. 2. The results presented in Fig. 2 show that the activity coefficient of the components is less than unity and the activity coefficient of Ti or Al increases with increasing its content, indicating that binary TiAl melts take on a negative deviation from the ideal solution. With increasing temperatures, each component's activity coefficient increases, and the activity coefficient — temperature relationship can be expressed as:

$$\ln \gamma_i = A + B/T \quad (8)$$

where  $A$  and  $B$  are constants, whose values can be obtained by regression analysis of the data presented in Fig. 2.

Tables 2 and 3 show the estimated coefficients  $A$

**Table 1** Basic properties and parameters of Ti and Al [12] (electronic charge, electronic density, mole volume and experimental constants)

Element	$\phi/V$	$n_{ws}/(d.u.)^{1/3}$	$V_m^{2/3}/\text{cm}^2$	$r/p$	$\mu$
Ti	3.65	1.47	4.8	1.0	0.04
Al	4.20	1.39	4.2	1.9	0.07

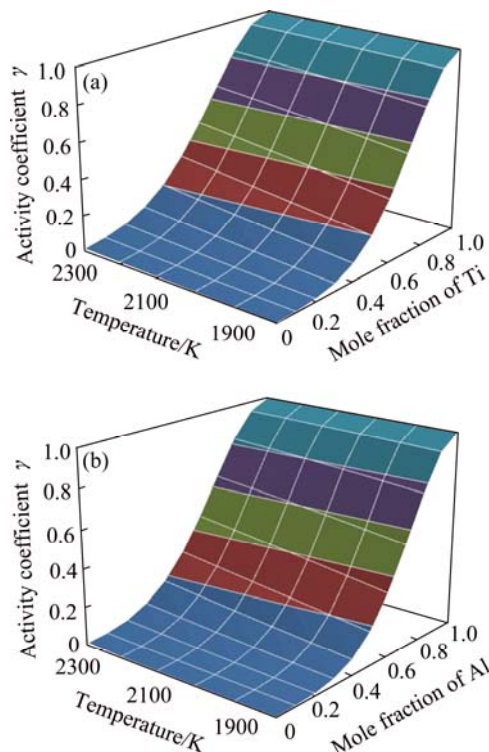


**Fig. 2** Activity coefficient — temperature — composition relationship for Ti (a) and Al (b) in binary TiAl alloys

and  $B$  for the activity coefficient—temperature relationships in TiAl alloys ( $0 \leq x(\text{Al}) \leq 0.5$ ) in a temperature range between 1800 and 2300 K. Thus, as a first approximation the activity coefficient—temperature relationship of the components in TiAl alloys is formulated.

**Table 2** Activity coefficient—temperature relationship for binary TiAl ( $0 \leq x(\text{Al}) \leq 0.5$ ) alloys ( $\ln \gamma(\text{Ti}) = A + B/T$ )

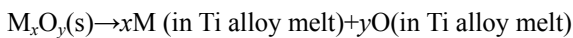
$x(\text{Al})$	$A$	$B$
0.1	0.027	-169.8
0.2	0.107	-672.1
0.3	0.237	-1495
0.4	0.418	-2633
0.5	0.648	-4075

**Table 3** Activity coefficient—temperature relationship for binary TiAl ( $0 \leq x(\text{Al}) \leq 0.5$ ) alloys ( $\ln \gamma(\text{Al}) = A + B/T$ )

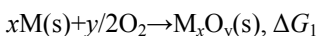
$x(\text{Al})$	$A$	$B$
0.1	2.252	-14132
0.2	1.763	-11123
0.3	1.354	-8520
0.4	0.996	-6262
0.5	0.691	-4347

### 3.2 Thermodynamics of interactions between oxide ceramics and Ti alloy melts

The interaction between oxide ceramics and TiAl melts is a complex physical and chemical process, and many researchers have studied the mechanisms of the interaction by experiments. Researches indicated that the most probable reason of alloy contamination is the dissolution of oxides by molten Ti alloys [9,16,17]. One possible mode of the interaction between Ti alloy melts and oxides ( $M_xO_y$ ) is the dissolution of M and atomic O in the melt by reaction:



Thus, for the investigation of the thermodynamics of interactions between oxide ceramics and Ti alloy melts, one should not only consider the stability of the oxide itself but also take into account of the solubility of the oxide in Ti alloy melts. The values of the Gibbs free energy of  $M_xO_y$  dissolution ( $\Delta G_f$ ) can be obtained by summatting the following reactions:



namely,

$$\Delta G_f = \Delta G_2 + \Delta G_3 - \Delta G_1 \quad (9)$$

where  $\Delta G_1$  is the standard Gibbs free energy of formation of corresponding oxides, as listed in Table 4 [18];  $\Delta G_2$  and  $\Delta G_3$  can be approximately obtained by thermodynamic calculation.

**Table 4** Standard Gibbs free energy of formation of chosen oxides [18]

Oxide	$\Delta G_f / (\text{kJ} \cdot \text{mol}^{-1})$
CaO	-795.378+195.06 $T$
Al <sub>2</sub> O <sub>3</sub>	-1682.927+323.24 $T$
MgO	-609.571+116.52 $T$
Y <sub>2</sub> O <sub>3</sub>	-1897.862+281.96 $T$

At a given temperature and composition, the Gibbs free energy of M dissolution reaction is expressed as [18]:

$$\Delta G_2 = x \sum a_i RT \ln \left( \frac{M_i}{100M_M} \gamma_M^0 \right) \quad (10)$$

where  $i$  is the component Ti or Al;  $a_i$  is the activity of  $i$ ,  $a_i = x_i \gamma_i$ ;  $x_i$  is the mole fraction of  $i$ ;  $\gamma_i$  is the activity coefficient of  $i$ , as shown in Fig. 2;  $M_i$  is the relative atomic mass of solvent  $i$ ;  $M_M$  is the relative atomic mass of solute M;  $\gamma_M^0$  is the coefficient of transformation between different activity standard states, whose value is approximate to unity for an ideal or almost ideal solution and  $10^{-3}$  for a non-ideal solution, respectively. At a given temperature and composition, the Gibbs free energy of O dissolution reaction is expressed as [18]:

$$\Delta G_3 = y \left( \sum x_i \Delta G_i + RT \sum x_i \ln \gamma_i \right) / 2 \quad (11)$$

where  $\Delta G_i$  is the Gibbs free energy of the oxygen dissolved in the pure  $i$  melt, whose value can be approximately obtained by thermodynamic data of binary Ti–O and Al–O systems [19–21],  $\Delta G_{\text{Ti}} \approx -21.5T$ ,  $\Delta G_{\text{Al}} \approx 23.4T$ . Using Eqs. (9)–(11) and taking one mole oxygen atom as the standard, the Gibbs free energy of  $M_xO_y$  dissolution can be written as:

$$\Delta G_f = \frac{1}{y} \left( \sum x_i R T x_i \gamma_i \ln \frac{M_i \gamma_M^0}{100 M_M} + \frac{y R T x_i \ln \gamma_i}{2} + \frac{y x_i \Delta G_i}{2} - \Delta G_1 \right) \quad (12)$$

According to Eq. (12) and thermodynamic data including activity coefficients in Tables 2 and 3, the Gibbs free energy of oxides in Ti alloy melts ( $0 \leq x(\text{Al}) \leq 0.5$ ) can be calculated. In this study, four common oxides (CaO, MgO, Al<sub>2</sub>O<sub>3</sub> and Y<sub>2</sub>O<sub>3</sub>) are selected for investigation. The calculated results of Gibbs free energy of these oxides in Ti alloy melts ( $0 \leq x(\text{Al}) \leq 0.5$ ) are shown in Fig. 3 at different temperatures.

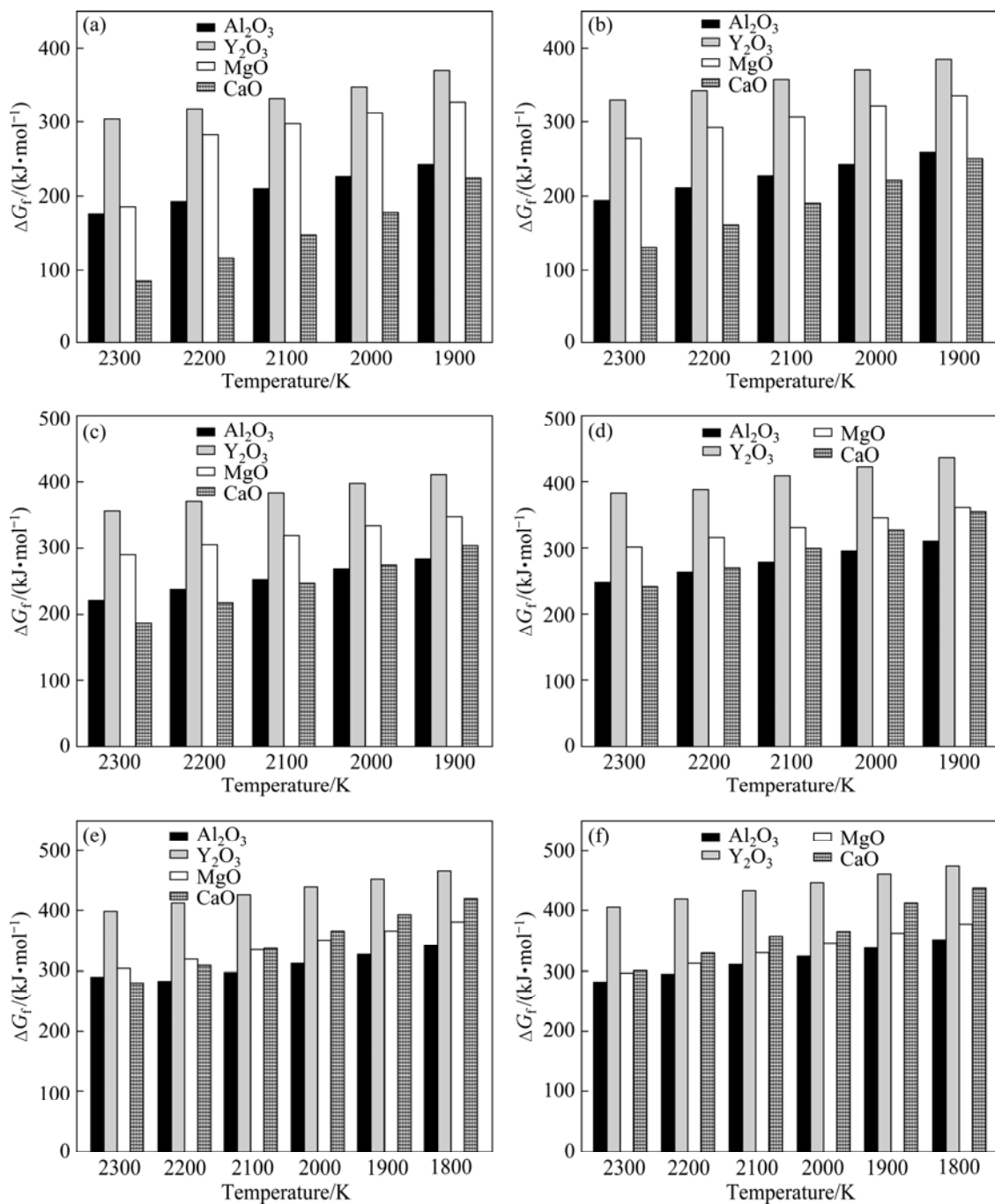


**Fig. 3** Calculated Gibbs free energy of four oxides in molten Ti and Ti alloys ( $0 \leq x(\text{Al}) \leq 0.5$ ) at different temperatures: (a) In Ti melts; (b) In Ti-10Al melts; (c) In Ti-20Al melts; (d) In Ti-30Al melt; (e) In Ti-40Al melt; (f) In Ti-50Al melt

At equilibrium, the Gibbs free energy of  $\text{M}_x\text{O}_y$  dissolution is expressed as:

$$\Delta G_f = -RT \ln K = -RT \ln \left( \frac{a_M^x \cdot a_O^y}{a_{\text{M}_x\text{O}_y}} \right) = -RT \ln \left( \frac{w(\text{M})^x w(\text{O})^y \cdot \gamma_{\text{M}}^x \gamma_{\text{O}}^y}{a_{\text{M}_x\text{O}_y}} \right) \propto -\ln w(\text{M}) \cdot w(\text{O}) \quad (13)$$

where  $T$  is the melt temperature;  $R$  is the mole gas constant;  $a$  is the chemical activity of components;  $K$  is the equilibrium constant;  $w(\text{M})$  and  $w(\text{O})$  are the mass fractions of M and O content in alloy melts. It can be seen from Eq. (13) that the impurity contents  $w(\text{M}) \cdot w(\text{O})$  are inversely proportional to the Gibbs free energy of  $\text{M}_x\text{O}_y$  dissolution ( $\Delta G_f$ ), namely,  $\ln w(\text{M})w(\text{O}) \propto -\Delta G_f$ . This indicates that the higher Gibbs free energy of oxides dissolution leads to the lower equilibrium dissolved impurity contents in alloy melts, consequently indicating

the higher thermodynamic stability of oxides. As shown in Fig. 3, both alloy composition and melt temperature are found to directly affect the Gibbs free energy for dissolution of oxides, thus affecting the stability of oxides.

For every figure in Fig. 3, it can be seen that the Gibbs free energy of oxide dissolution is decreased with increasing the melt temperature, indicating that the stability of the oxide decreases with increasing the temperature. This is mainly due to the decrease of Ti and Al activities in melts with decreasing the melt temperature (in Fig. 2), and the chemical reactivity of the melts depends on the activities of Ti and Al elements in melts. Therefore, by decreasing the melt temperature, the chemical reactivity of the melt is directly decreased, and consequently increases the stability of the oxide.

By the comparison of figures in Fig. 3, it can be seen that at the same melt temperature, the Gibbs free energy for dissolution of four oxides increases with increasing the Al content, indicating that the stability of oxides increases with increasing the Al content in the alloy. This is mainly due to the decrease of the activity of Ti with increasing the Al content (in Fig. 2(a)), and the activity changes of Ti directly affect the chemical reactivity of the melts, considering that the chemical reactivity of Ti is higher than that of Al. Therefore, with increasing the Al content of the alloy, the chemical activity of the alloy melt is directly decreased, and consequently increases the stability of the oxide.

In the last two decades, TiAl alloys have attracted attention as potential candidates for high-temperature structural applications in the aerospace, military automotive industry. At the present stage, the main factors to limit the manufacture of mass market TiAl components are the low ductility. Researches so far indicate that the interstitial O content directly affects the room temperature ductility of TiAl alloys. Generally, it is accepted that the oxygen content in cast TiAl alloys should not exceed technically acceptable limit of about  $1 \times 10^{-3}$ . This suggests that one should select oxides with high values of  $\Delta G_f$  as crucible or mould for melting or casting Ti alloys to reduce the alloy contamination. According to the calculated composition–temperature–stability relationship for selected oxides, one can very easily differentiate the relative stability of oxides against Ti alloys with different compositions. For the cast TiAl alloys, the melt temperature is generally lower than 2000 K. Therefore, the order of decreasing stability follows the sequence: when  $x(\text{Al}) \leq 0.2$ ,  $\text{Y}_2\text{O}_3 > \text{MgO} > \text{Al}_2\text{O}_3 > \text{CaO}$ ; when  $0.2 < x(\text{Al}) \leq 0.3$ ,  $\text{Y}_2\text{O}_3 > \text{MgO} > \text{CaO} > \text{Al}_2\text{O}_3$ ; when  $0.3 < x(\text{Al}) \leq 0.5$ ,  $\text{Y}_2\text{O}_3 > \text{CaO} > \text{MgO} > \text{Al}_2\text{O}_3$ , in agreement with the experimental results of KUANG et al [17] by melting experiments.

### 3.3 Experimental analysis of interactions between $\text{Y}_2\text{O}_3$ ceramics and Ti alloy melts

According to above thermodynamic analysis, one can know that  $\text{Y}_2\text{O}_3$  has the highest thermodynamic stability. Therefore, as a representative of evaluated oxides,  $\text{Y}_2\text{O}_3$  is selected as crucible materials to run melting experiments of Ti–Al alloys in this work, and the melting result is quantitatively analyzed, as described in Section 2.1.

Figure 4 shows the results of chemical composition analysis of Ti alloy ingots with different Al contents. As shown in Fig. 4, taking into account of the initial oxygen concentration of the master alloy, the oxygen contents of the ingots exposed to the  $\text{Y}_2\text{O}_3$  crucibles are higher than that value, and the oxygen content decreases with increasing the Al content in Ti alloys, in agreement with thermodynamic calculations. By comparison of figures in Fig. 3, the Gibbs free energies of dissolution of four oxides increase with increasing the Al content, indicating that the stability of oxides increases with increasing the Al content in the alloy. This is mainly due to the decrease of the Ti activity with increasing the Al content (Fig. 2(a)), resulting in the weakening of its interaction with the oxide and consequently the decrease of the alloy contamination. Therefore, it is expected that the addition of alloying elements (such as Nb and Cr), which not only improves the comprehensive properties of the alloy but also reduces the Ti activity and decreases the chemical reactivity of the alloy, can help to reduce the oxide–alloy interactions and the alloy contamination. Under the processing conditions used in this work, the oxygen enrichment in Ti alloy melts proportionally increases with increasing the Al content. Regression analysis of experimental data in Fig. 4, yields an equation in the form:

$$w(\text{O}) = -0.233x(\text{Al}) + 0.1695 \quad (14)$$

The regression coefficient of this fit is  $R^2 = 0.99$ ,

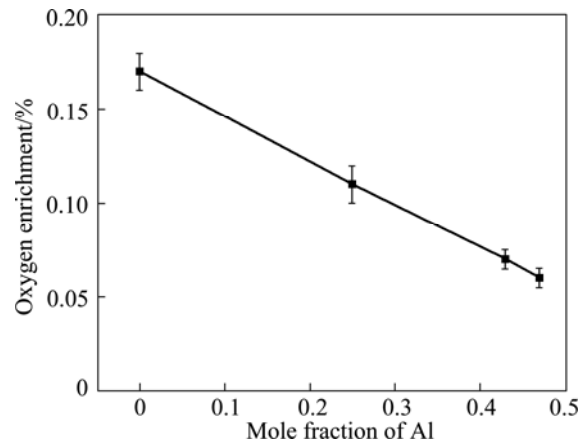


**Fig. 4** Results of chemical analysis showing oxygen enrichment of molten Ti alloys with different Al contents at 1973 K

indicating a good linear relationship between  $w(O)$  and  $x(Al)$ .

Figure 5 shows the results of chemical composition analysis of Ti–47Al alloy ingots at different melt temperatures. As shown in Fig. 5, taking into account of the initial oxygen concentration of the master alloy, the oxygen contents of the ingots exposed to the  $Y_2O_3$  crucibles are higher than that value, and the oxygen enrichment increases with increasing the melt temperature, in agreement with the thermodynamic calculations. As shown in Fig. 3(f), the Gibbs free energy values of dissolution of four oxides decrease with increasing the melt temperature, indicating that the stability of oxides decreases with increasing the melt temperature. This is mainly due to the increase of Ti and Al activities in melts with increasing the melt temperature (Fig. 2), resulting in the enhancement of its interaction with the oxide and consequently the increase of the alloy contamination. These findings indicate that the decrease of the melt temperature helps to reduce the oxide–alloy interactions and the alloy contamination. For the processing conditions used in this work, the oxygen enrichment in Ti alloy melts proportionally increases with increasing the melt temperature. Regression analysis of the experimental data in Fig. 5 yields an equation in the form:

$$w(O)_{Ti-47Al} = 0.0002T - 0.3346 \quad (15)$$

The regression coefficient of this fit is  $R^2=0.99$ , indicating a good linear relationship between  $w(O)$  and  $T$ .

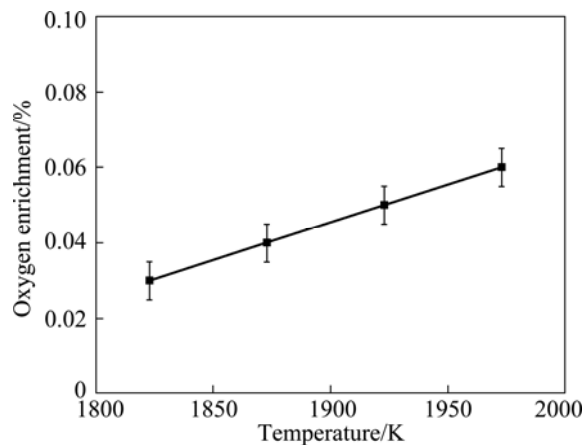


**Fig. 5** Result of chemical analysis showing oxygen enrichment of molten Ti alloys with different melt temperatures

## 4 Conclusions

1) According to the predicting results of thermodynamic stability of oxides  $CaO$ ,  $MgO$ ,  $Al_2O_3$  and  $Y_2O_3$  in molten Ti and Ti alloys, it was found that the stability of oxides increased with increasing the Al

content in the alloy and decreasing the melt temperature. According to the calculated composition–temperature–stability relationship for evaluated oxides, the order of decreasing stability follows the sequence: when  $x(Al) \leq 0.2$ ,  $Y_2O_3 > MgO > Al_2O_3 > CaO$ ; when  $0.2 < x(Al) \leq 0.3$ ,  $Y_2O_3 > MgO > CaO > Al_2O_3$ ; when  $0.3 < x(Al) \leq 0.5$ ,  $Y_2O_3 > CaO > MgO > Al_2O_3$ .

2) According to the thermodynamic analysis,  $Y_2O_3$  was found to have the highest thermodynamic stability among the evaluated oxides. As a representative of the evaluated oxides,  $Y_2O_3$  was selected as crucible materials to run melting experiments of Ti–Al alloys. The melting result was quantitatively analyzed. The results showed that at the same experimental conditions, the oxygen enrichment in Ti alloys proportionally decreased with increasing the Al content in Ti alloys, indicating that the oxide–alloy interaction was reduced with increasing the Al content. For the same alloy composition, the decrease of the melt temperature helps to reduce the oxide–alloy interactions and the alloy contamination.

## References

- BOYER R R. An overview on the use of titanium in aerospace industry [J]. Materials Science and Engineering A, 1996, 213: 103–114.
- SAHA R L, NANDY T K, MISRA R D K, JACOB K T. On the evaluation of stability of rare earth oxides as face coats for investment casting of titanium [J]. Metallurgical and Materials Transactions B, 1990, 21: 559–566.
- KIM Y W. Gamma titanium aluminides: Their status and future [J]. JOM, 1995, 7: 39–41.
- DING Hong-sheng, GUO Jing-jie, JIA Jun, WANG Chun-yi. Thermodynamic stability of molding materials for casting Ti–6Al–4V alloy [J]. Journal of Harbin Institute of Technology, 1999, 6(2): 56–59.
- LIU Ai-hui. The interfacial reaction law and micromechanism between titanium alloy melts and ceramic mould [D]. Harbin: Harbin Institute of Technology, 2007. (in Chinese)
- CHEN Yu-yong, XIAO Shu-long, KONG Fan-tao, WANG Xue. Microstructure and interface reaction of investment casting TiAl alloys [J]. Transactions of Nonferrous Metals Society of China, 2006, 16: 1910–1914.
- LUO Wen-zhong, SHEN Jun, MIN Zhi-xian, FU Heng-zhi. Investigation of interfacial reactions between TiAl alloy and crucible materials during directional solidification process [J]. Rare Metal Materials and Engineering, 2009, 38: 1441–1445. (in Chinese)
- LI Bang-sheng, LIU Ai-hui, NAN Hai, BI Wei-sheng, GUO Jing-jie, FU Heng-zhi. Wettability of TiAl alloy melt on ceramic moulds in electromagnetic field [J]. Transactions of Nonferrous Metals Society of China, 2008, 18: 518–522.
- JIA Qing, CUI Yu-you, YANG Rui. A study of two refractories as mould materials for investment casting TiAl based alloys [J]. Journal of Materials Science, 2006, 41: 3045–3049.
- LIU Ai-hui, LI Bang-sheng, NAN Hai, SUI Yan-wei, GUO Jing-jie, FU Heng-zhi. Study of interfacial reaction between TiAl alloys and four ceramic molds [J]. Rare Metal Materials and Engineering, 2008, 37: 956–959. (in Chinese)
- ZHU Yan, YANG Yan-qing, SUN Jun. Calculation of activity coefficients for components in ternary Ti alloys and intermetallics as

matrix of composites [J]. Transactions of Nonferrous Metals Society of China, 2004, 14: 875–879.

[12] GUO Jing-jie, SU Yan-qing. The thermodynamic and kinetic analysis of Ti alloys during the ISM process [M]. Harbin: Harbin Institute of Technology Press, 1998. (in Chinese)

[13] DING Xue-yong, FAN Peng, HAN Qi-yong. Models of activity and activity interaction parameter in ternary metallic melt [J]. Acta Metallurgica Sinica, 1994, 30(2): 49–59. (in Chinese)

[14] DING Xue-yong, WANG Wen-zhong. A new thermodynamic calculation formula for activity of component in binary system [J]. Acta Metallurgica Sinica, 1994, 30(10): 444–447. (in Chinese)

[15] MIDEMA A R, DE CHATEL P F, DE BOER F R. Cohesion in alloys fundamentals of a semi-empirical model [J]. Physica B, 1980, 100: 1–28.

[16] BARBOSA J, RIBEIRO C S, MONTEIRO A C. Influence of superheating on casting of  $\gamma$ -TiAl [J]. Intermetallics, 2007, 15: 945–955.

[17] KUANG J P, HARDING R A, CAMPBELL J. Investigation into refractories as crucible and mould materials for melting and casting  $\gamma$ -TiAl alloys [J]. Materials Science and Technology, 2000, 16: 1007–1016.

[18] HUANG Xi-gu. Metallurgical principles [M]. Beijing: Metallurgical Industry Press, 1989. (in Chinese)

[19] WALDNER P. Modelling of oxygen solubility in titanium [J]. Scripta Materialia, 1999, 40: 969–974.

[20] CANCAREVIC M, ZINKEVICH M, ALDINGER F. Thermodynamic modeling of the system titanium-oxygen [J]. Calphad, 2007, 31: 330–342.

[21] DAS K, CHOUDHURY P, DAS S. The Al–O–Ti (Aluminum–oxygen–titanium) system [J]. Journal of Phase Equilibria, 2002, 23: 525–536.

## Ti–Al 合金熔体与氧化物 陶瓷界面反应的热力学分析

崔仁杰, 唐晓霞, 高 明, 张 虎, 宫声凯

北京航空航天大学 材料科学与工程学院 空天材料与服役教育部重点实验室, 北京 100191

**摘要:** 研究  $\text{CaO}$ 、 $\text{MgO}$ 、 $\text{Al}_2\text{O}_3$  和  $\text{Y}_2\text{O}_3$  与熔融 Ti 及 Ti 合金之间的界面反应热力学。根据氧化物在 Ti 合金熔体中的溶解反应机制建立热力学模型, 通过热力学分析预测各氧化物相对于  $\text{Ti}-\text{Al}(0 \leq x(\text{Al}) \leq 0.5)$  合金的热力学稳定性。根据氧化物坩埚熔炼实验结果来研究氧化物与  $\text{Ti}-x\text{Al}$  合金熔体的界面反应, 对熔炼效果进行定量分析, 发现随着合金中 Al 含量的提高和熔体温度的降低, 合金中杂质元素含量成比例的减少, 这与氧化物稳定性计算结果一致。

**关键词:** Ti 合金; 热力学; 氧化物陶瓷; 界面反应

(Edited by YANG Hua)